Martin et al., https://doi.org/10.1083/jcb.201604015

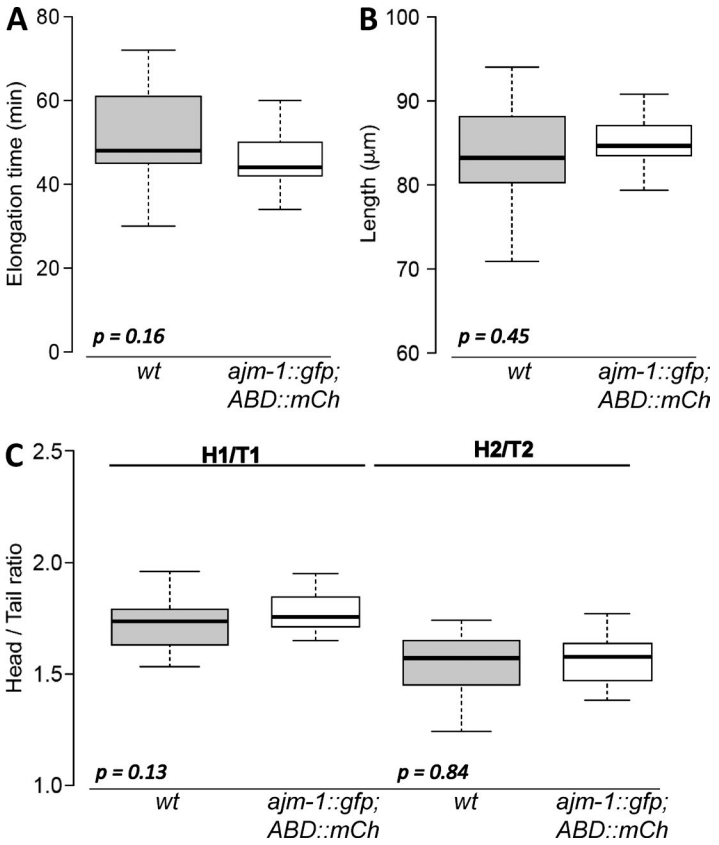

Figure S1. ***ajm-1::GFP; vab-10(ABD)::mCherry*–carrying embryos develop as wt animals.** (A–C) Box plot representing early elongation time (A), length of the embryos at the end of early elongation (B), and head-to-tail width ratio at 1.2-fold (H1/T1) and at the end of early elongation (H2/T2; C) in wt and *ajm-1::GFP; abd::mCherry*. Box plots represent the minimum, maximum, 25th, 50th (median), and 75th percentiles of the population. *t* test p-values are indicated on the graph. This study revealed that transgenic animals expressing AJM-1::GFP and the F-actin binding probe VAB-10(ABD)::mCherry display elongation rates similar to those of wt embryos (A). The length of transgenic and wt embryos is also similar at the end of early elongation, when body wall muscles start contracting (B). Moreover, the morphology of these embryos is similar, with similar head-to-tail width ratios at the beginning (H1/T1) and end (H2/T2) of early elongation. For details on the method used to generate these data, refer to Martin et al. (2014, 2016). $n > 40$ embryos were analyzed per genotype.

THE JOURNAL OF CELL BIOLOGY

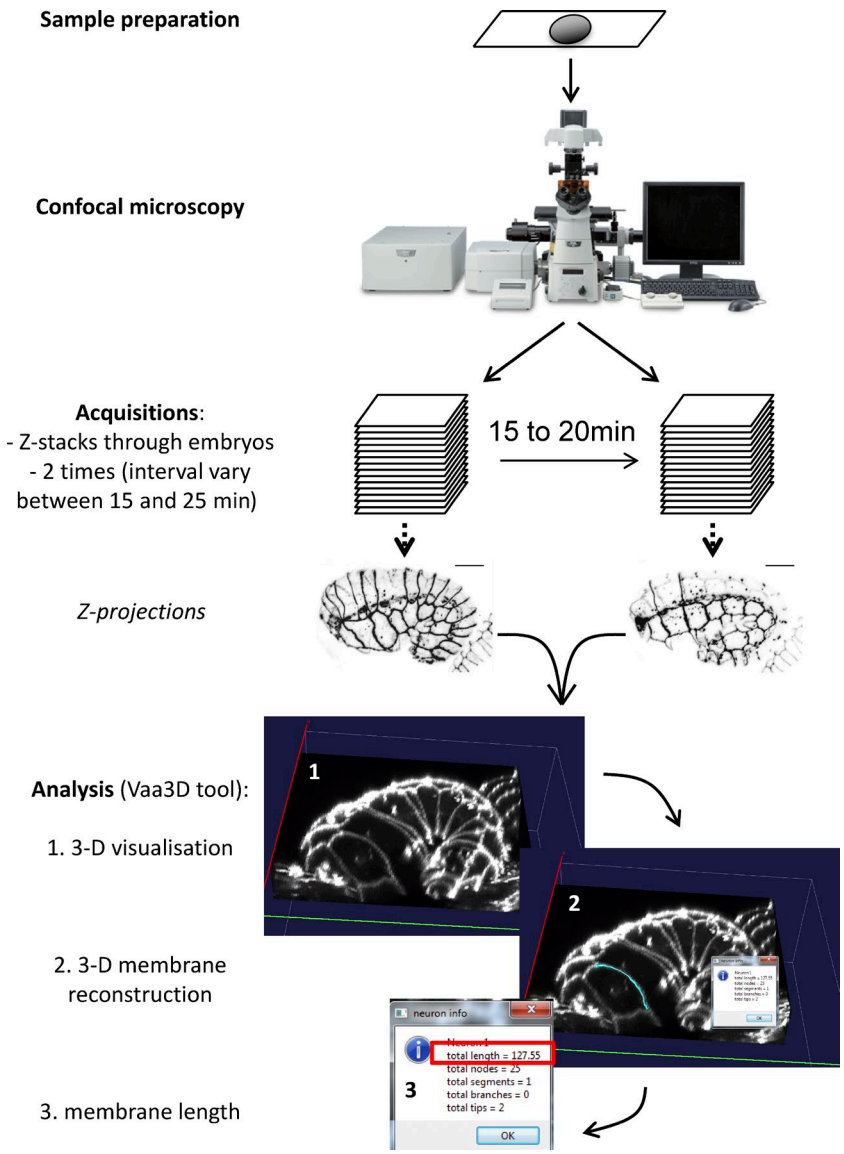

Figure S2. **Step-by-step method to quantify junction elongation rates.** Embryos were mounted on an agarose pad and observed using pinpoint confocal microscopy. *z*-stacks covering the entire width of the embryos were recorded at the beginning of early elongation (comma stage) and after 15–20 min, being sure that the second measurement was made before the body wall muscles started contracting. *z*-stacks were analyzed using Vaa3D tools. This analysis included resampling of images and 3D reconstruction. Vaa3D linear object identification and measurement tools in 3D were used to measure the length of cell–cell junctions between two identified vertices. As previously reported, 3D measurements of cell–cell junctions are more accurate than measurements of junctions observed in a *z*-projection of *z*-stacks (Kang et al., 2015).

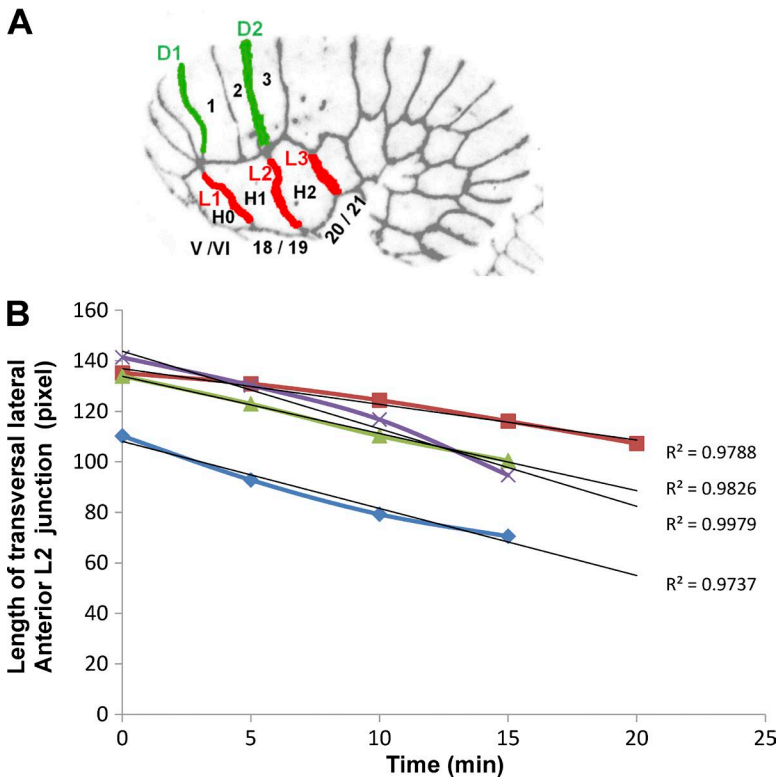

Figure S3. **Deformation rate of transversal L2 junctions measured for *n* = 4 different wt embryos.** L2 was measured every 5 min during early elongation. This study revealed that the deformation rate of L2 is constant during early elongation.

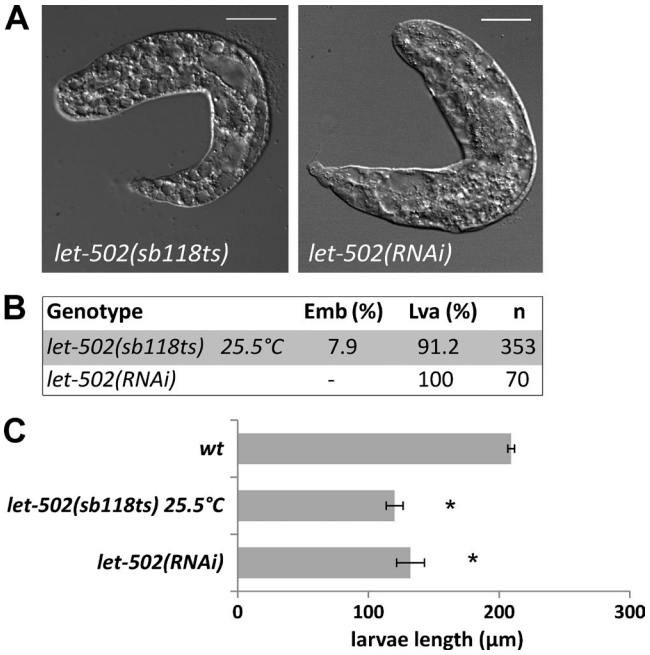

Genotype		Emb (%)	Lva (%)	n
let-502(sb118ts)	*25.5°C*	7.9	91.2	353
let-502(RNAi)		-	100	70

Figure S4. ***let-502(RNAi)*–treated animals display defects similar to *let-502(sb118ts)* mutants grown at nonpermissive temperature.** (A) Arrested larvae observed for *let-502(sb118ts)* mutants grown at 25.5°C and *let-502(RNAi)*–treated animals grown at 20°C upon differential interference contrast illumination. (B) Percentage of embryonic lethality (Emb) and larval arrest (Lva) in *let-502(sb118ts)* and *let-502-(RNAi)*. (C) Bar graph representing the mean length of larvae in wt, *let-502(sb118ts)*, and *let-502-(RNAi)*. *t* test p-value <0.05. Error bars indicate SEM. *n* > 40 larvae were analyzed per genotype.

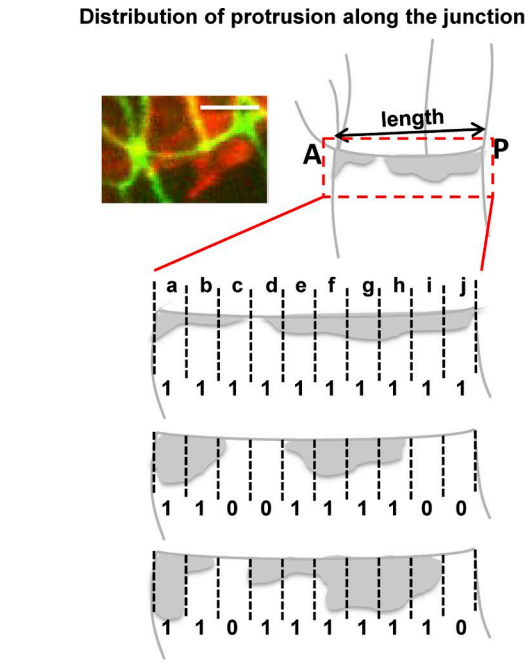

	a	b	c	d	e	f	g	h	i	j
Σ	3	3	1	2	3	3	3	3	2	1
N	3	3	3	3	3	3	3	3	3	3
%	100	100	33	66	100	100	100	100	66	33

Σ: sum of positive cases ("1")
N: sum of positive and negative cases ("1" and "0")
% (distribution): Σ/N

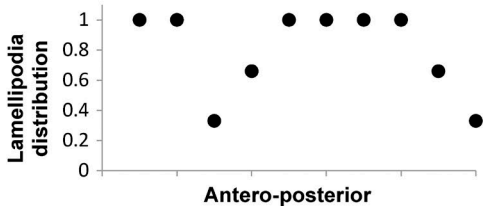

Figure S5. **Method used to quantify the distribution of protrusions along the junction between D1/L1 and D2/L2 vertices.** In brief, cell–cell junctions located between D1/L1 and D2/L2 vertices were divided into 10 equal sections. The presence of a protrusion was identified for each section at 24 different time points for four different embryos. We computed the distribution as the percentage of positive events (Σ) per measurement per section (*N*), and plotted this distribution (bottom). A Fisher equal test (computed using R statistical tools) was used to assess how surprising it is to witness a reduction or increase of the distribution of protrusions at a given section for a given mutant compared with wt embryos. Bars: 10 µm; (enlarged images) 5 µm.

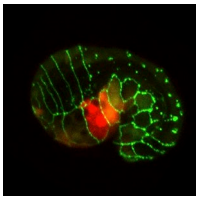

Video 1. **Transfer of H2 cytoplasm to the amoeboid protrusion.** Pulses of blue-light illumination of H2 lateral cells induced the photoconversion of Kaede GFPs expressed under the control of the hypodermic-specific lin-26p promoter into strong RFPs. This spectral isolation of H2 allowed us to observe the transfer of part of its cytoplasm into a unique and deep protrusion located at the dorsal part of the cell.

References

Kang, S., C.Y. Lee, M. Gonçalves, A.D. Chisholm, and P.C. Cosman. 2015. Tracking epithelial cell junctions in *C. elegans* embryogenesis with active contours guided by SIFT flow. *IEEE Trans. Biomed. Eng.* 62:1020–1033. http://dx.doi.org/10.1109/TBME.2014.2319236

Martin, E., S. Harel, B. Nkengfac, K. Hamiche, M. Neault, and S. Jenna. 2014. pix-1 controls early elongation in parallel with mel-11 and let-502 in *Caenorhabditis elegans*. *PLoS One.* 9:e94684. http://dx.doi.org/10.1371/journal.pone.0094684

Martin, E., O. Rocheleau-Leclair, and S. Jenna. 2016. Novel metrics to characterize embryonic elongation of the nematode *Caenorhabditis elegans*. *J. Vis. Exp.* 28:e53712. http://dx.doi.org/10.3791/53712